

## Assessment of photovoltaic module temperature estimation for four years with four different software

*Dört yıllık fotovoltaik modül sıcaklık tahmininin dört farklı yazılımla değerlendirilmesi*

Doga TOLGAY<sup>\*1,2,3</sup> , Muhammet Samet YAKUT<sup>2,3</sup> , Talat OZDEN<sup>3,4</sup> , Bulent G. AKINOGLU<sup>1,3,5</sup> 

<sup>1</sup>Middle East Technical University (METU), Faculty of Arts and Science, Department of Physics, 06800, Ankara

<sup>2</sup>Middle East Technical University (METU), Faculty of Engineering, Department of Electrical and Electronics Engineering, 06800, Ankara

<sup>3</sup>The Center for Solar Energy Research and Applications (ODTU-GUNAM), Middle East Technical University (METU), 06800, Ankara

<sup>4</sup>Gumushane University, Faculty of Engineering, Department of Energy Systems Engineering, 29100, Gumushane

<sup>5</sup>Middle East Technical University (METU), Earth System Science Program, 06800, Ankara

• Received: 01.04.2022

• Accepted: 21.10.2022

### Abstract

The software used today, on the estimation of module temperature of photovoltaic systems, seem very important to be analyzed. These estimates are crucial in future techno-economic and environmentally friendly analyses of the systems to reach better achievements for future generations. This is very important to reach lifetime analyses of long-term feasibility to find out payback time and the levelized cost of energy. The present work is based on this issue, to test the module temperature estimation formulas used by four commonly used software models, and to determine the most suitable software for temperature analyses of five different photovoltaic modules in Middle Anatolia. Outdoor truthful long-term testing is the main realistic approach to reach fundamental contemplations. After an introductory basic knowledge, the main materials and methods are discussed to enlighten the analysis. The main methodology is given and further prospects are enlightened. Four well-known software are analyzed using four years of outdoor testing of five different photovoltaic modules. Measured ambient temperature and solar irradiance are used in the categorization of the software estimation performances. PV\*SOL appears to be superior at low irradiance and ambient temperature, whereas Helioscope appears to be superior overall.

**Keywords:** Photovoltaic module temperature, PV correlations, Solar cell, Solar energy, Temperature estimation

### Öz

Günümüzde kullanılan fotovoltaik sistemlerde modül sıcaklığını tahminleme yazılımlarının analiz edilmesi çok önemlidir. Bu tahminler ileriye yönelik tekno-ekonomik ve çevre duyarlı analizler için gelecek nesiller için daha kazanımlı olacaktır. Mevcut çalışma, bu konuyla ilgili olarak, yaygın kullanılan dört yazılım modeli tarafından kullanılan modül sıcaklık tahmin formüllerini test etmek ve Orta Anadolu'da beş farklı fotovoltaik modülün sıcaklık analizleri için en uygun yazılımı belirlemektir. Açık alanda yapılan tutarlı ve uzun dönemli testler, temel sonuçlara ulaşmak için en gerçekçi yaklaşımdır. Giriş bölümünde temel bilgilerin ardından, analize ışık tutacak temel materyal ve yöntemler tartışılmaktadır. Ana metodoloji verilmekte ve sonuçlar sunulmaktadır. Dört iyi bilinen yazılım, beş farklı fotovoltaik modülün dört yıllık açık alan testleri kullanılarak analiz edilmiştir. Yazılım tahmin performanslarının sınıflandırılmasında ortam sıcaklığı ve güneş ışınımı kullanılmıştır. PV\*SOL, düşük ışınım ve ortam sıcaklığında üstün görünürken, Helioscope genel olarak daha iyi sonuçlar vermiştir.

**Anahtar kelimeler:** Fotovoltaik modül sıcaklığı, PV korelasyonları, Güneş hücresi, Güneş enerjisi, Sıcaklık tahmini

\* Doga TOLGAY; doga.tolgay@mail.utoronto.ca

## 1. Introduction

The problems with the Earth's environment are mainly due to the use of conventional energy sources. The increasing demand for energy while co-saving the Planet drives the motion for the adaptation of clean and sustainable energy sources. Renewable energy sources such as hydro, wind, and solar seem the world's new energy supply. As of 2010, the total installed renewable energy capacity was 1.2 TW; in 2019, it was 2.5 TW, which is doubled in 9 years at an increasing pace. In 2019 the installed Solar photovoltaics was around 580 GW, whereas this number was simply 40 GW in 2010 ([International Renewable Energy Agency, 2020](#)).

The photovoltaic installation capacity will continue exponentially to increase all over the world. Therefore, comprehensive testing of the PV performance in outdoor conditions is crucial to get the best efficiency and yield. R/D on PV and the operating temperature of PV modules seem very important as it affects both the panels' efficiency and their degradation rates. This issue of degradation rates is still heavily studied, especially in new next-generation solar cell systems ([Ozden, Akinoglu, et al., 2018](#)). It should also be noted that the operation of PV modules under outdoor conditions in diverse climates results in different performance outcomes ([Ozden, Carr, et al., 2020](#)).

The efficiency of the modules varies seasonally due to variation of a plane-of array (POA) irradiance, ambient temperature, and wind speed. It was demonstrated that the performances of thin-film modules vary seasonally depending on the light and temperature exposure ([Nikolaeva-Dimitrova et al., 2010](#)). ([J. Ye et al., 2012](#)) observed the seasonal efficiency for a-Si single-junction, Monocrystalline Silicon and Micromorph cells vary. Both modules attained their highest efficiencies during the Monsoon season when module temperatures attain their minimum values due to seasonal variations and heavy rainfall. They observed that relative changes in monthly outdoor efficiency within the year were around 3.1%, 2.7%, and 1.6% for mono-Si, micromorph, and a-Si, respectively. Moreover, dust accumulation in summer makes the efficiency more prone to diminish in summer compared with winter. ([Jha & Tripathy, 2019](#)) indicated that the efficiency reduction in summer is 7.5% whereas, in winter, the efficiency reduction is 4.9% and also analyzed the thermal behavior of the modules using a 3D computational model based on the finite element method.

Most of the energy incident from the Sun is either not absorbed effectively or not converted to produce photocurrent. Non-absorbed photons and electrons excited to high levels in the conduction band produce heat in their relaxation. The heat generation within the cell reduces the efficiency of the modules by creating hot carriers. It is observed that 72% of incident energy was converted into heat, causing an increase adversely in the cell temperature rather than creating a usable form of energy ([Shen et al., 2020](#)). It is well known that the results of the power output and module temperature are inversely related ([Dubey et al., 2013](#)). Furthermore, ([Radziemska, 2003](#)) observed that the output power change is  $-0.65 \text{ \%}/\text{K}$  which affects the change in efficiency as  $-0.08 \text{ \%}/\text{K}$  according to the experiments conducted on the crystalline silicon solar cell. ([Rahman et al., 2015](#)) observed that  $-0.06 \text{ \%}/\text{°C}$  change in efficiency for the monocrystalline PV module.

([Aly et al., 2019](#)) demonstrated the variation of the cell temperature concerning the ambient temperature, POA irradiance, and wind speed. The variation of operating cell temperature seems linear with respect to the ambient temperature up to POA irradiance of  $800 \text{ W}/\text{m}^2$ . On the other hand, the change in cell temperature is outlined to be hyperbolic with respect to wind speed variations. However, not only the wind speed but also the wind direction and tilt angle are the other two critical parameters for the module temperature analysis ([Tuncel et al., 2020](#)). ([Jaszczur et al., 2019](#)) demonstrated the importance of the tilt angle by analyzing the temperature distribution within the cell for several inclinations. It was observed that polycrystalline-silicon PV modules attained their highest temperature when it was parallel to the surface, whereas when the angle is  $15^\circ$  the module temperature was lower, because of the unavailability of cooling due to wind when inclination was zero.

The correlation between the module temperature and POA irradiance is also linked to the technology of the module ([Atse et al., 2017](#)). Different modules react diversely in outdoor conditions. ([Z. Ye et al., 2013](#)) analyzed the module temperature of sixteen different PV modules, manufactured using four different technologies, and observed that although the value of module temperature was varying, the trends were relatively similar. They stated that the difference between the module and the ambient temperature starts to increase as the ambient temperature increases, having the poly-Si concrete solar cell had the least

temperature difference between ambient and module temperatures, whereas the highest difference was attained at the  $\mu$ -Si module.

In our previous works (Ozden, Tolgay, et al., 2018, 2020) it is observed that the module temperature could reach above 60 °C in a moderate climate in the middle of Anatolia, Ankara. In our previous study (Ozden, Tolgay, et al., 2020), all analyses were conducted on ten different module temperature estimations schemes without specifically considering the effect of ambient temperature, solar irradiance, and their seasonal variations. It is concluded that both intrinsic and extrinsic parameters should be considered to estimate the module temperature accurately. The ambient temperature, wind speed, and irradiance are the most used parameters with form-based heat and wind coefficients. The difference between our previous study and this study is previously ten correlation equations are used and two of them are found to be perform better than others, whereas in this study the most commonly used four software is analyzed by considering different weather conditions separately. The two best equations are proposed by (King et al., 2004) and (Skoplaki et al., 2008).

To reach accurately the estimation schemes which is very important for long-term techno-economic analysis (Karaveli et al., 2018; Ozden, et al., 2020)) to find out truthfully the efficiency and yield the software in hand as: HOMER, Helioscope, PVsyst, and PV\*SOL (Folsom Labs, 2019; HOMER Software, 2019; PVsyst, 2019; Valentin Software, 2019) are detailly studied. The present work comprehensively achieves to be as an original stand work in PV temperatures with the temperature estimation formulas developed by several authors (Duffie et al., 1985; Faiman, 2008; King et al., 2004; Skoplaki et al., 2008).

This study, starting from the methodology, compares the module temperatures obtained in outdoor conditions using the four most utilized software as stated above. We obtained essential data on meteorological and systems properties measurements for four years. The data and the methodology we integrated are gathered in the cold and semi-arid climate of Ankara, Turkey. We believe that the works in the present research and the methodology will firmly clarify the outdoor testing of the behavior of the module temperatures to inform the investors and researchers by giving clear findings. This study's novelty is that the 16 different weather categories are studied to determine the most suitable temperature estimation for four different software.

The importance of module temperature estimation lies in the fact that software uses these estimations to predict the yield and efficiency of modules. Accurately predicted module temperature will present more authentic estimations for the performance of photovoltaic modules. Additionally, this paper aims to determine the better-correlated procedure for each weather category and temperature estimation formula for five-module types in Ankara, which leads to the construction of a feasible and trustworthy techno-economic analysis. In this study, the ambient temperature and incoming solar irradiance values are also evaluated to analyze and discuss the module temperature estimation schemes. Considering that this study is done in the Middle Anatolia, our results are expected to be valid for the "Csb" Koppen climate classified regions.

## 2. Materials and methods

### 2.1. Description sites and modules

The tested PV modules are located on the rooftop of the Department of Physics, METU in Ankara, which is in the Central Anatolia Region of Turkey. The exact location of latitude and longitude of our outdoor test platform are 39.9° N and 32.8° E. The altitude of the platform is 929 m, and modules are mounted with a tilt angle of 32° tilt and 0° azimuth angle so facing directly South. Figure 1 is the picture of the outdoor installations of the tested modules. The modules were installed in April 2012, and the tested modules have been operating since. However, this research will consider the data taken out between January 2017 and December 2020.

We investigated five different types of PV modules in this study which are Copper Indium Selenide (CIS), Monocrystalline Silicon (Mono-Si), Polycrystalline Silicon (Poly-Si), amorphous silicon ( $\mu$ -Si/a-Si), and Heterojunction with Intrinsic Thin layer (HIT) structures (Figure 1). Technical details of the PV modules investigated are presented in Table 1. The values are taken from the datasheets given by the companies producing the modules. Mono-Si, Poly-Si, and HIT modules have mono- and poly-crystalline silicon

structures, whereas the other two are composed of thin-film PV of different compositions. All modules are cleaned once a week.



**Figure 1.** Configuration of ODTÜ-GÜNAM outdoor test facility (a) and tested modules – 1: CIS, 2: Poly-Si, 3: Mono-Si, 4:  $\mu$ c-Si/a-Si, 5: HIT (b)

**Table 1.** Module nameplate values

Module Types	$P_{MAX}$ [W]	$V_{OC}$ [V]	$I_{SC}$ [A]	$V_{MPP}$ [V]	$I_{MPP}$ [A]	$\eta$ [%]	$\beta_{STC}$ [%/°C]	$T_{m,NOCT}$ [°C]	Area [m <sup>2</sup> ]
<b>CIS</b>	130.0	59.50	3.28	44.90	2.90	12.3	-0.39	40	1.05
<b>Mono-Si</b>	160.0	43.70	5.06	35.30	4.58	12.5	--**	--**	1.28
<b>Poly-Si</b>	130.0	21.70	8.18	17.80	7.30	12.7	-0.45*	46	1.02
<b><math>\mu</math>c-Si / a-Si</b>	128.0	59.80	3.45	45.40	2.82	9.1	-0.24	44	1.40
<b>HIT</b>	230.0	42.30	7.22	34.30	6.71	16.5	-0.30	45	1.39

\* The parameter unit is %/K. \*\* There is no datasheet for this module. Therefore, some results are missing.

The climate of Middle Anatolia can be defined within the Köppen – Geiger climate classification system (Peel et al., 2007; Rubel et al., 2017) as a semi-arid desert. The average ambient temperature is given for four years as 14.8 °C. The highest and lowest daily temperatures are recorded as 39.8 °C and -6.1 °C on 3 July 2017 and 3 January 2017, respectively. Further information about the measured meteorological climatic parameters and highest, lowest, and average values of solar irradiance values are tabulated in Table 2. These measurements are taken using a weather station installed on the ODTÜ-GÜNAM outdoor test facility.

The module and ambient temperature, solar irradiation, and electrical performance were recorded via a PV analyzer. The average values of the data were recorded every ten minutes. T-type thermocouples were used in the measurement of ambient temperature, and solar irradiation was measured by a high precision secondary standard Kipp & Zonnen pyranometer. The thermocouples were fixed to the middle of the backside of the PV modules. As an exception, the temperature sensor of the  $\mu$ c-Si/a-Si module was set close to its junction box, which is in the middle of the top of the backside (Ozden, Tolgay, et al., 2018).

Ambient temperature, relative humidity, precipitation, solar irradiance, and both speed and direction of the wind were measured by using the meteorological station. The station and PV analyzer recorded and stored the averaged data every ten minutes. The pyranometer and meteorological station were located at the top of the roof, and incoming solar radiation and wind speed were not obstructed by any other nearby elements.

**Table 2.** Meteorological statistics

	2017	2018	2019	2020
<b>T<sub>amb,average</sub> [°C]</b>	14.41	15.49	14.82	15.29
<b>T<sub>amb,highest</sub> [°C]</b>	39.85 (3 July)	36.63 (17 August)	38 (14 August)	40.67 (3 September)
<b>T<sub>amb,lowest</sub> [°C]</b>	-6.11 (3 January)	-5.22 (27 December)	-5.04 (9 January)	-1.59 (17 January)
<b>Precipitation Average [mm]</b>	0.061	0.118	0.079	0.067
<b>Precipitation Highest [mm]</b>	155.6	202.2	288	245.2
<b>Precipitation Lowest [mm]</b>	0	0	0	0
<b>I<sub>t,average</sub> [W/m<sup>2</sup>]</b>	211.39	210.84	200.24	225.9
<b>I<sub>t,highest</sub> [W/m<sup>2</sup>]</b>	1381.1 (7 May)	1404.5 (19 January)	1350.4 (4 July)	1273.6 (6 April)
<b>I<sub>t,lowest</sub> [W/m<sup>2</sup>]</b>	-7.73 (3 August)	-9.6 (10 June)	-6.93 (15 August)	-9.93 (8 October)
<b>V<sub>wind,average</sub> [m/s]</b>	0.96	0.89	0.85	0.84
<b>V<sub>wind,highest</sub> [m/s]</b>	12.1	13	11.6	13
<b>V<sub>wind,lowest</sub> [m/s]</b>	0	0	0	0

### 2.3. Methods

**Table 3.** Temperature models used by four different software

Equation #	Correlation	Software
1	$T_c = \frac{T_a + (T_{c,NOCT} - T_{a,NOCT}) \left( \frac{G_T}{G_{NOCT}} \right) \left[ 1 - \frac{\eta_{STC}(1 - \alpha_p T_{c,STC})}{\tau \alpha} \right]}{1 + (T_{c,NOCT} - T_a) \left( \frac{G_T}{G_{NOCT}} \right) \left( \frac{\alpha_p \eta_{STC}}{\tau \alpha} \right)}$	HOMER
2	$T_c = G_T (e^{a+b*WS}) + T_a$	Helioscope
3	$T_c = T_a + G_T * \frac{\alpha(1 - \eta_{STC})}{U_0 + U_1 * WS}$	PVsyst
4	$T_c = T_a + k * \frac{G_T}{G_{NOCT}}$	PV*SOL

Three of the given temperature models include many parameters. For explanations of these parameters, one can refer to the Nomenclature, whereas some of the parameters are taken from different references as explained below. Equations (1) and (3),  $\eta_{STC}$  refers to the efficiency of a module at standard test conditions, and  $\alpha_p$  is the temperature coefficient. Both  $\eta_{STC}$  and  $\alpha_p$  are taken from the datasheets of the PV modules. In addition to this, in equation (1),  $\tau \alpha$  is taken as 0.9 (Eckstein, 1990; Sandnes & Rekstad, 2002).  $a$  and  $b$  in equation (2) are empirically determined parameters, and they depend on the module type. In other words,  $a$  and  $b$  are taken as -3.97 and -0.0594 for glass/cell/glass & open rack module structure and, -3.56 and -0.075 for other modules which are composed of glass/cell/polymer sheet & open rack (King et al., 2004). The wind speed in equation (2) is fixed at 10 m in height. To convert our wind speed measurements to 10 m reference height, the following law is used (Twidell & Weir, 2015):

$$\frac{WS}{WS_{ref}} = \left( \frac{z}{z_{ref}} \right)^n \quad (5)$$

in which  $n$  refers to friction coefficient which depends on the topography of the test site. According to Bañuelos-Ruedas et al. it is taken as 0.3 because the topography of our test site can be described as a small town with some trees and shrubs (Bañuelos-Ruedas et al., 2010).  $z_{ref}$ ,  $z$ , and  $WS_{ref}$  are reference heights measured from the ground of the outdoor test platform, 10 m, and wind speed at the outdoor test platform.

$U_0$  and  $U_1$  in equation (3) are the thermal coefficients describing the effect of the solar radiation on PV cell temperature, and the cooling effect of the wind, respectively (Koehl et al., 2011). They are taken as 23.09 and 3.11 for the CIS module while for other modules they are taken as 25 and 6.84 (Faiman, 2008; Koehl et al., 2011).

According to PV\*SOL documentation (Valentin Software, 2019),  $k$  strongly depends on the installation type of PV modules. Since PV modules in the test site can be considered as free-standing installation,  $k$  is taken as 20 for all PV modules.

The module temperature calculation for the Mono-Si module using the Homer temperature estimation formula requires knowledge of the datasheet values of this module. The unavailability of this information resulted in the missing values in Table 5.

In the present work, the effects of ambient temperature and solar irradiance are considered in detail. Since this study aims to obtain how close the temperature models estimate the cell temperature under different conditions, 16 different categories are generated according to different ambient temperature and solar irradiation intervals. The details about the contents of these categories are supplied in Table 4.

**Table 4.** Description of categories

	$0 \leq I_t < 300$	$300 \leq I_t < 700$	$700 \leq I_t < 900$	$900 \leq I_t$
$T_{amb} < 0$	C1	C5	C9	C13
$0 \leq T_{amb} < 10$	C2	C6	C10	C14
$10 \leq T_{amb} < 25$	C3	C7	C11	C15
$25 \leq T_{amb}$	C4	C8	C12	C16

The main thermal parameter is the difference between the estimated and measured module temperature

$$\Delta T_i = T_{estimated,i} - T_{measured,i} \quad (6)$$

where  $i$  is just an indexing number,  $T_{estimated,i}$  and  $T_{measured,i}$  are the estimated module temperature by the methodology and measured module temperature in our outdoor test facility, respectively.

Error calculation is needed to understand how good temperature models are estimating the module temperature. Root mean squared error (RMSE) and mean bias error (MBE) methods are used to obtain error values. These two statistical errors are the main parameters to determine the accuracy of estimation schemes of the methodologies (Akinoglu, 1991). Although both RMSE and MBE are concerned with the deviations between estimated and measured module temperature values, their focus is different. RMSE focuses on the wild deviations between estimated and measured values, and more sensitive to high deviations than the MBE, whereas MBE measures over or under-estimations. These two error calculation methods can be expressed as follows:

$$MBE = \frac{1}{N} \sum_{i=1}^N \Delta T_i \quad (7)$$

$$RMSE = \sqrt{\frac{1}{N} \sum_{i=1}^N (\Delta T_i)^2} \quad (8)$$

where  $N$  denotes the total number of data and,  $i$  is just an indexing number.

### 3. Results and discussion

Estimation of the above-mentioned parameters is only possible with the correct assessment of the module temperatures. Implicit and explicit parameters are being used by temperature estimation formulas. The former involves the heat transfer coefficients, thermal loss coefficients, thermal and physical properties, and maximum efficiency whereas, the latter contains the incoming irradiance and ambient temperature.

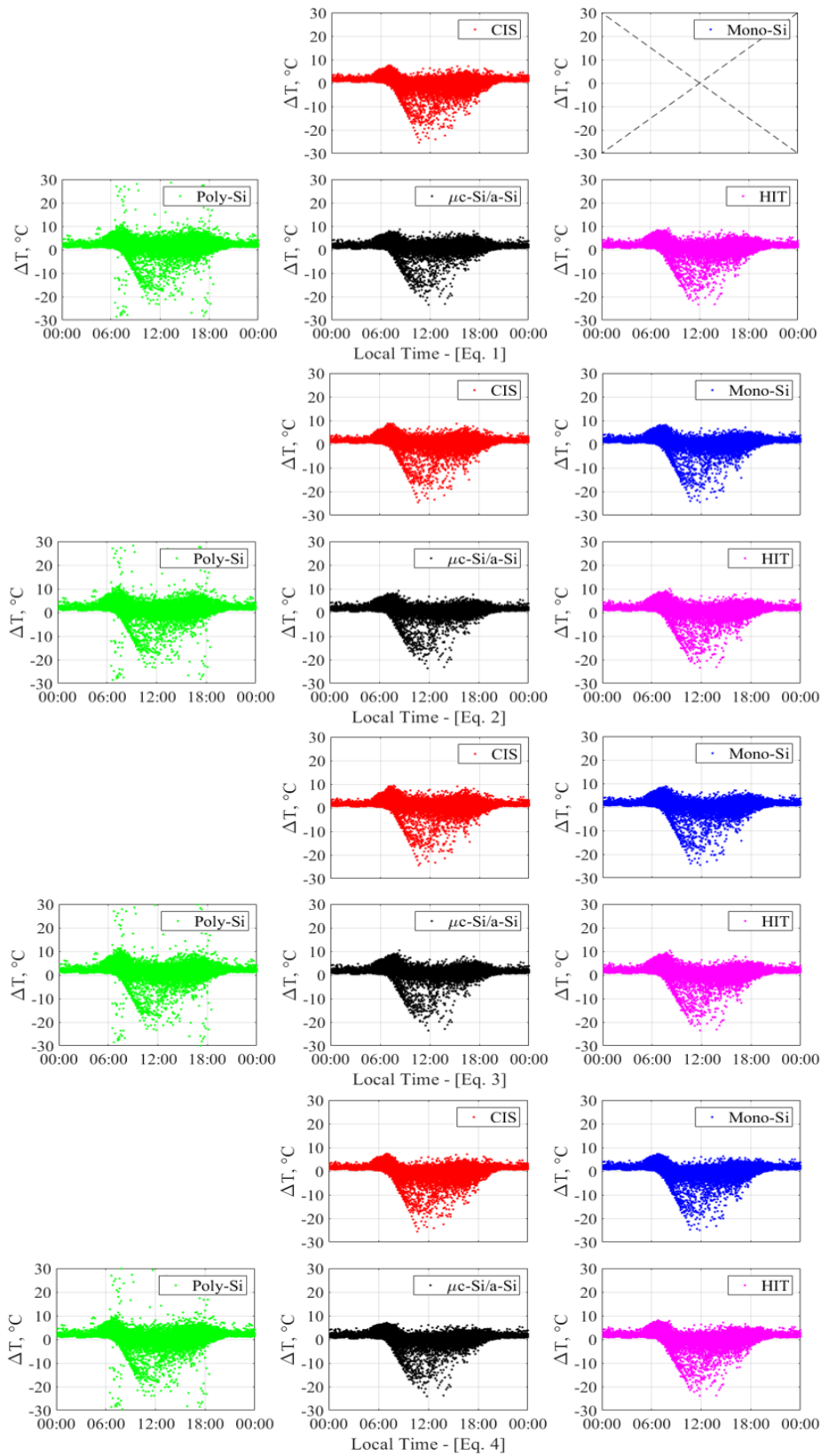


**Figure 2.** Results of category 3 [Irradiation:  $0 \leq I_t < 300 \text{ W/m}^2$ , Temperature:  $10 \leq T_{\text{amb}} < 25 \text{ }^\circ\text{C}$ ] for Eq. 1, Eq. 2, Eq. 3 and Eq. 4

Deviations are measured by considering equation (6), if the  $\Delta T$  is positive, the software overestimates the module temperature, whereas if  $\Delta T$  is negative, the module temperature is underestimated. The deviations are plotted and categorized according to the categories listed in Table 4. For each category, there exist four

graph groups that correspond to the specific equation. By considering all results, the deviations between the estimated and measured temperature can reach up to  $-30\text{ }^{\circ}\text{C}$  and  $+30\text{ }^{\circ}\text{C}$  (Figures 2 and 3).

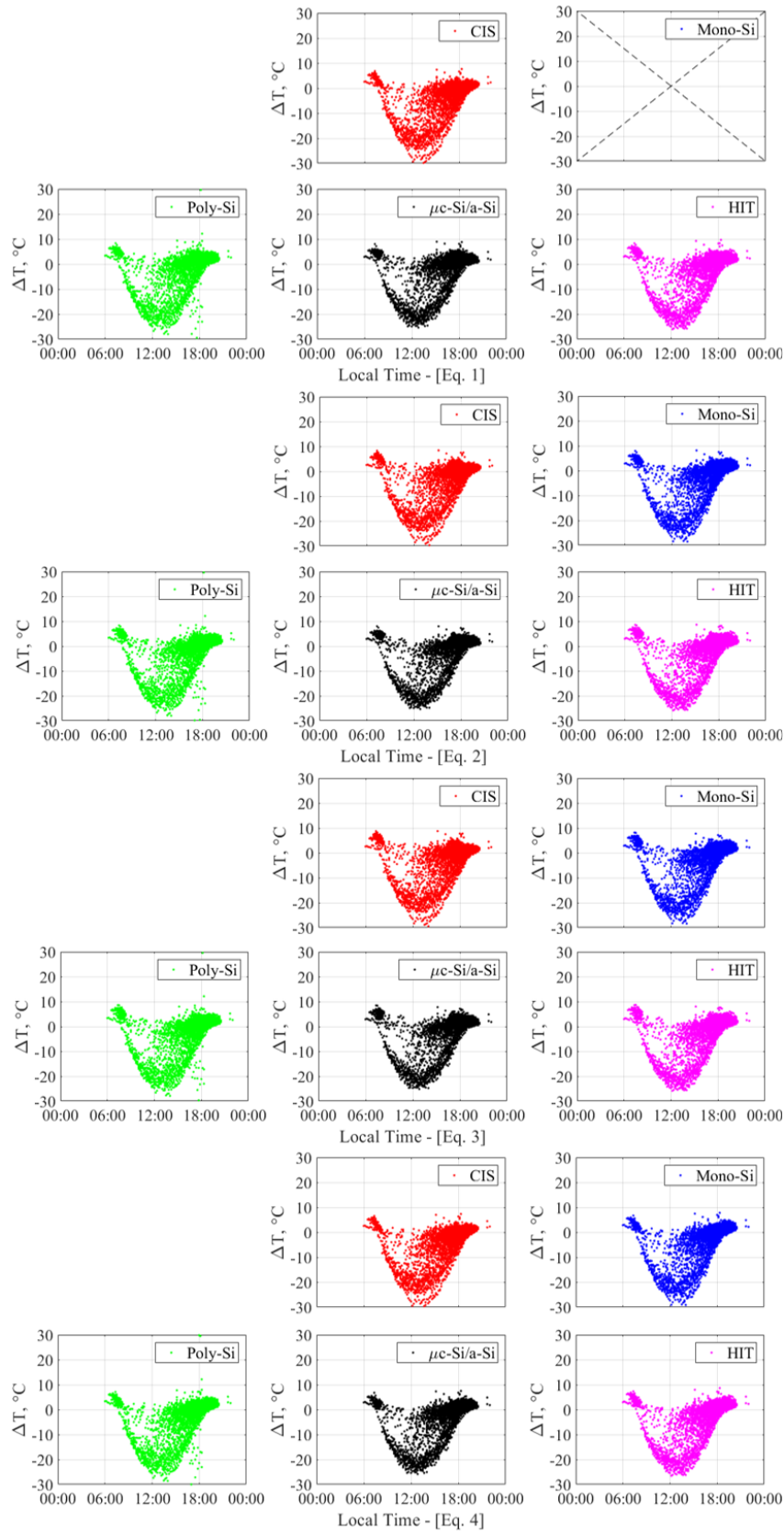


**Figure 3.** Results of category 4 [Irradiation:  $0 \leq I_t < 300\text{ W/m}^2$ , Temperature:  $25\text{ }^{\circ}\text{C} \leq T_{amb}$ ] for Eq. 1, Eq. 2, Eq. 3 and Eq. 4

Results demonstrate that for different meteorological conditions, the reaction of the modules considerably alters. The software that made the best estimations by considering RMSE and MBE for different categories was listed in Table 5 a, b, c, and d. Table 5 is categorized according to Table 4. Every category has the names of the five methodologies of module temperature estimation in the first column. The first four blocks of Table 5 part a are for the irradiance range of 0 - 300 W/m<sup>2</sup> and the latter blocks of b, c, and d are for the irradiance value ranges of 300 - 700 W/m<sup>2</sup>, 700-900 W/m<sup>2</sup>, and larger than 900 W/m<sup>2</sup>, respectively. As also can be observed that each block of benches is for the module temperature ranges of  $T_{amb} < 0\text{ }^{\circ}\text{C}$ ,  $0\text{ }^{\circ}\text{C} < T_{amb} < 10\text{ }^{\circ}\text{C}$ ,  $10\text{ }^{\circ}\text{C} < T_{amb} < 25\text{ }^{\circ}\text{C}$  and  $25\text{ }^{\circ}\text{C} < T_{amb}$ . The green-colored boxes are the better estimation schemes while the reds are the weaker.

It can be determined that for the lower irradiance values of 0-300 W/m<sup>2</sup> the methodology of PV\*SOL is better up to module temperatures of 25 °C. However, larger than 25 °C, PV\*SOL is the weakest for the three types of modules and still weak for the other two. This suggests that this methodology is weaker for quite higher ranges of module temperatures which can be attributed to its development stage of the utilized measured values to construct the formalism. PVsyst has rather better values for CIS type modules, but it resembles the weakest estimations in general for this small range of irradiance values (0 - 300 W/m<sup>2</sup>). However, we should note that for this range, the better results are interestingly evenly distributed within the methodologies under discussion. The results of our analyses show that, as can be observed to some extent, the weaker and better methodologies are rather evenly distributed for higher irradiance values. Except for this determination for PV\*SOL is the unique temperature range of  $0\text{ }^{\circ}\text{C} < T_{amb} < 10\text{ }^{\circ}\text{C}$  for the irradiance values larger than 900 W/m<sup>2</sup> (Table 5.d). Although this can be attributed to the extent of the evaluated data in hand, it can also be thought to be the better estimation scheme of this methodology for a rather smaller range of  $0\text{ }^{\circ}\text{C} < T_{amb} < 10\text{ }^{\circ}\text{C}$ . However, also should be stated to be under discussion is the increasing weaker estimation of PV\*SOL since it still quite better estimation schemes at lower irradiance values (see the parts b and c of Table 5).

Every model uses solar radiation flux on module plane ( $G_T$ ), Helioscope and PVsyst are considering the relation between it with module parameter and wind speed, whereas HOMER does not include wind speed as a parameter in its model. On the other hand for the PV\*SOL,  $G_T$  and installation coefficient (k) are multiplicative factors with each other. This emphasizes the direct effect of installation type on the estimated temperature. As wind speed increases the overall effect of the  $G_T$  decreases in Helioscope and PVsyst, suggesting these two parameters cannot be considered separately. Although PVsyst and Helioscope have similar estimations under high irradiances, the latter model offers a closer estimation below 700 W/m<sup>2</sup> in Table 5. At low irradiance, the best estimations are done by PV\*SOL that does not use wind speed or module parameters. This hints the utilization of the wind speed or module parameters can result in a deviation between estimation and measurement at low irradiance. Nonetheless, at high irradiance values, the module parameters and wind speed decrease the errors in estimations. The importance of the parameters depends on the module technology and requires future investigations.

An important remark that we obtained on the presented results is quite a good evaluation of the methodologies widely used by the investors and researchers. In this discussion, we also need to add that, for the higher solar irradiance larger than 300 W/m<sup>2</sup>, the tabulated results should be carefully handled for future investigations.

But a final note is that for the larger values of solar irradiance, the methodology used by Helioscope is better than a general consideration.

**Table 5.** The best/worst estimations of methods for MBE and RMSE values for various categories solar irradiance vs temperature (a, b, c and d); values of the green colored boxes are better, and reds are weaker.**(a) Irradiance: 0 – 300 W/m<sup>2</sup>**

		CIS	Mono-Si	Poly-Si	µc-Si/a-Si	HIT	
<b>T<sub>amb</sub> &lt; 0 °C</b>	<b>C1</b>						
	Homer	MBE	1.64	--	3.04	2.18	1.73
		RMSE	2.38	--	3.91	2.85	3.68
	Helioscope	MBE	2.11	1.11	2.99	2.11	1.77
		RMSE	2.86	3.59	3.90	2.80	3.72
	PVsyst	MBE	2.25	1.17	3.04	2.23	1.74
	RMSE	3.03	3.64	3.97	2.99	3.74	
	PV*SOL	MBE	1.56	0.76	2.63	1.75	1.41
		RMSE	2.32	3.54	3.61	2.39	3.57
<b>0 ≤ T<sub>amb</sub> &lt; 10 °C</b>	<b>C2</b>						
	Homer	MBE	1.12	--	2.74	1.97	1.89
		RMSE	2.21	--	3.66	2.64	2.84
	Helioscope	MBE	1.74	1.55	2.67	1.87	1.94
		RMSE	2.59	2.60	3.62	2.59	2.91
	PVsyst	MBE	1.93	1.64	2.74	2.05	1.92
	RMSE	2.77	2.70	3.72	2.80	2.94	
	PV*SOL	MBE	1.00	1.07	2.18	1.39	1.45
		RMSE	2.18	2.37	3.29	2.21	2.60
<b>10 ≤ T<sub>amb</sub> &lt; 25 °C</b>	<b>C3</b>						
	Homer	MBE	0.94	--	2.52	2.02	2.06
		RMSE	2.78	--	6.60	3.07	3.26
	Helioscope	MBE	1.66	1.63	2.37	1.87	2.07
		RMSE	3.07	3.03	6.56	2.99	3.32
	PVsyst	MBE	1.89	1.70	2.44	2.05	2.02
	RMSE	3.23	3.14	6.62	3.18	3.35	
	PV*SOL	MBE	0.78	1.06	1.81	1.30	1.50
		RMSE	2.77	2.82	6.39	2.69	3.00
<b>25 °C &lt; T<sub>amb</sub></b>	<b>C4</b>						
	Homer	MBE	-2.01	--	-0.16	-0.16	-0.18
		RMSE	6.15	--	6.40	5.95	6.14
	Helioscope	MBE	-1.37	-0.72	-0.50	-0.49	-0.33
		RMSE	6.00	6.37	6.40	5.93	6.14
	PVsyst	MBE	-1.16	-0.77	-0.55	-0.42	-0.50
	RMSE	5.97	6.38	6.41	5.95	6.15	
	PV*SOL	MBE	-2.20	-1.19	-0.97	-0.96	-0.8
		RMSE	6.21	6.41	6.43	5.94	6.14

**(b) Irradiance: 300 – 700 W/m<sup>2</sup>**

		CIS	Mono-Si	Poly-Si	µc-Si/a-Si	HIT	
<b>T<sub>amb</sub> &lt; 0 °C</b>	<b>C5</b>						
	Homer	MBE	0.23	--	4.24	6.54	4.19
		RMSE	4.50	--	5.54	7.17	5.38
	Helioscope	MBE	3.00	2.00	3.07	5.28	3.72
		RMSE	5.10	3.74	4.54	5.98	4.90
	PVsyst	MBE	3.93	2.04	3.08	5.76	3.23
	RMSE	5.70	3.99	4.76	6.71	4.77	
	PV*SOL	MBE	-0.41	0.05	1.12	3.32	1.77
		RMSE	4.55	3.53	3.79	4.31	3.86
<b>0 ≤ T<sub>amb</sub> &lt; 10 °C</b>	<b>C6</b>						
	Homer	MBE	-0.97	--	3.18	4.11	2.52
		RMSE	4.20	--	4.84	5.05	4.23
	Helioscope	MBE	2.42	1.31	2.59	3.48	2.68
		RMSE	4.43	3.48	4.30	4.42	4.21
	PVsyst	MBE	3.51	1.69	2.95	4.37	2.47
	RMSE	5.13	3.89	4.74	5.38	4.31	
	PV*SOL	MBE	-1.68	-1.37	-0.08	0.79	-0.01
		RMSE	4.46	3.85	3.80	3.05	3.51

		<b>C7</b>		<b>CIS</b>	<b>Mono-Si</b>	<b>Poly-Si</b>	<b>μc-Si/a-Si</b>	<b>HIT</b>	
		MBE	RMSE						
<b>10 ≤ T<sub>amb</sub> &lt; 25 °C</b>	Homer	MBE		-1.60	--	2.46	3.09	1.77	
		RMSE		4.04	--	9.34	4.26	3.74	
	Helioscope	MBE		1.72	0.51	1.65	2.29	1.75	
		RMSE		3.84	3.20	9.06	3.46	3.62	
	PV <sub>syst</sub>	MBE		2.79	0.76	1.87	3.05	1.40	
		RMSE		4.46	3.50	9.17	4.22	3.70	
	PV*SOL	MBE		-2.41	-2.15	-0.99	-0.37	-0.91	
		RMSE		4.46	4.10	9.12	2.96	3.5	
			<b>C8</b>		<b>CIS</b>	<b>Mono-Si</b>	<b>Poly-Si</b>	<b>μc-Si/a-Si</b>	<b>HIT</b>
	<b>25 °C &lt; T<sub>amb</sub></b>	Homer	MBE		-1.99	--	2.18	3.10	1.76
RMSE				4.17	--	4.67	4.38	3.73	
Helioscope		MBE		1.04	0.20	0.82	1.81	1.24	
		RMSE		3.65	3.19	4.03	3.27	3.29	
PV <sub>syst</sub>		MBE		2.01	0.06	0.66	2.17	0.52	
		RMSE		4.10	3.37	4.16	3.63	3.26	
PV*SOL		MBE		-2.91	-2.16	-1.54	-0.56	-1.12	
		RMSE		4.7	4.13	4.47	3.14	3.53	

**(c) Irradiance: 700 – 900 W/m<sup>2</sup>**

		<b>C9</b>		<b>CIS</b>	<b>Mono-Si</b>	<b>Poly-Si</b>	<b>μc-Si/a-Si</b>	<b>HIT</b>	
		MBE	RMSE						
<b>T<sub>amb</sub> &lt; 0 °C</b>	Homer	MBE		-4.40	--	2.50	8.57	2.51	
		RMSE		7.95	--	6.00	9.18	5.88	
	Helioscope	MBE		-0.07	-1.28	-0.01	5.97	1.23	
		RMSE		5.25	4.28	3.97	6.32	3.86	
	PV <sub>syst</sub>	MBE		1.36	-1.72	-0.49	6.27	-0.07	
		RMSE		5.26	4.22	3.81	6.81	3.39	
	PV*SOL	MBE		-5.58	-4.24	-2.97	3.01	-1.73	
		RMSE		8.68	7.12	6.30	4.48	5.68	
			<b>C10</b>		<b>CIS</b>	<b>Mono-Si</b>	<b>Poly-Si</b>	<b>μc-Si/a-Si</b>	<b>HIT</b>
	<b>0 ≤ T<sub>amb</sub> &lt; 10 °C</b>	Homer	MBE		-2.61	--	3.04	5.63	2.20
RMSE				6.10	--	5.81	7.08	4.88	
Helioscope		MBE		2.58	0.20	1.48	4.05	1.91	
		RMSE		5.45	3.77	4.35	5.26	3.93	
PV <sub>syst</sub>		MBE		4.25	0.43	1.67	5.09	1.21	
		RMSE		6.42	4.1	4.71	6.33	3.89	
PV*SOL		MBE		-3.86	-3.81	-2.52	0.04	-2.10	
		RMSE		6.73	6.01	5.52	4.23	4.81	
		<b>C11</b>		<b>CIS</b>	<b>Mono-Si</b>	<b>Poly-Si</b>	<b>μc-Si/a-Si</b>	<b>HIT</b>	
<b>10 ≤ T<sub>amb</sub> &lt; 25 °C</b>		Homer	MBE		-3.18	--	2.27	4.33	1.63
	RMSE			5.77	--	6.39	5.80	4.40	
	Helioscope	MBE		2.03	-0.47	0.68	2.84	1.37	
		RMSE		4.67	3.78	5.47	4.05	3.73	
	PV <sub>syst</sub>	MBE		3.71	-0.23	0.87	3.9	0.66	
		RMSE		5.62	4.07	5.68	5.07	3.84	
	PV*SOL	MBE		-4.56	-4.64	-3.46	-1.33	-2.80	
		RMSE		6.63	6.41	6.91	4.06	4.96	
			<b>C12</b>		<b>CIS</b>	<b>Mono-Si</b>	<b>Poly-Si</b>	<b>μc-Si/a-Si</b>	<b>HIT</b>
	<b>25 °C &lt; T<sub>amb</sub></b>	Homer	MBE		-2.61	--	2.58	4.40	2.03
RMSE				5.09	--	6.30	5.60	4.15	
Helioscope		MBE		2.15	-0.37	0.41	2.40	1.22	
		RMSE		4.5	3.40	5.43	3.61	3.27	
PV <sub>syst</sub>		MBE		3.69	-0.60	0.14	2.97	0.08	
		RMSE		5.44	3.70	5.61	4.21	3.28	
PV*SOL		MBE		-4.13	-4.16	-3.38	-1.41	-2.57	
		RMSE		6.02	5.73	6.67	3.73	4.45	

**(d) Irradiance: > 900 W/m<sup>2</sup>**

		CIS	Mono-Si	Poly-Si	μc-Si/a-Si	HIT	
0 ≤ T <sub>amb</sub> < 10T <sub>amb</sub> < 0 °C	<b>C13</b>						
	Homer	MBE	-1.46	--	6.72	13.15	7.20
		RMSE	5.58	--	7.56	13.29	7.78
	Helioscope	MBE	0.96	-0.86	0.45	6.81	2.48
		RMSE	4.11	2.41	2.32	7.60	3.20
	PVsyst	MBE	2.12	-2.92	-1.65	5.47	-0.43
		RMSE	4.49	3.74	2.87	6.63	2.20
	PV*SOL	MBE	-2.95	-1.37	-0.06	6.30	1.97
		RMSE	6.13	3.7	3.47	6.63	3.54
	<b>C14</b>						
	Homer	MBE	1.79	--	8.39	11.41	6.78
		RMSE	8.90	--	12.22	13.9	10.70
Helioscope	MBE	6.88	3.15	4.81	7.84	4.82	
	RMSE	11.37	8.77	9.64	11.02	9.19	
PVsyst	MBE	8.67	2.57	4.18	8.18	3.16	
	RMSE	12.72	8.84	9.63	11.70	8.55	
PV*SOL	MBE	0.16	-0.36	1.29	4.32	1.30	
	RMSE	8.59	8.13	8.39	8.52	7.89	
10 ≤ T <sub>amb</sub> < 25 °C	<b>C15</b>						
	Homer	MBE	-2.71	--	3.79	6.35	2.28
		RMSE	6.46	--	7.64	7.71	5.48
	Helioscope	MBE	3.00	-0.54	0.91	3.64	1.08
		RMSE	6.15	4.83	6.25	4.94	4.56
	PVsyst	MBE	4.87	-0.84	0.54	4.29	-0.35
		RMSE	7.32	5.35	6.6	5.79	4.89
	PV*SOL	MBE	-4.49	-4.93	-3.47	-0.76	-3.31
		RMSE	7.39	7.27	7.46	4.38	5.98
	<b>C16</b>						
	Homer	MBE	-2.87	--	2.97	5.42	2.38
		RMSE	5.77	--	6.80	6.57	4.73
Helioscope	MBE	2.74	-0.65	0.02	2.74	1.14	
	RMSE	5.28	3.78	5.67	3.89	3.54	
PVsyst	MBE	4.55	-1.13	-0.51	3.22	-0.45	
	RMSE	6.45	4.19	5.88	4.46	3.64	
PV*SOL	MBE	-4.78	-5.10	-4.43	-1.73	-3.31	
	RMSE	6.92	6.68	7.53	4.09	5.25	
25 °C < T <sub>amb</sub>	<b>C13</b>						
	Homer	MBE	-1.46	--	6.72	13.15	7.20
		RMSE	5.58	--	7.56	13.29	7.78
	Helioscope	MBE	0.96	-0.86	0.45	6.81	2.48
		RMSE	4.11	2.41	2.32	7.60	3.20
	PVsyst	MBE	2.12	-2.92	-1.65	5.47	-0.43
		RMSE	4.49	3.74	2.87	6.63	2.20
	PV*SOL	MBE	-2.95	-1.37	-0.06	6.30	1.97
		RMSE	6.13	3.7	3.47	6.63	3.54
	<b>C14</b>						
	Homer	MBE	1.79	--	8.39	11.41	6.78
		RMSE	8.90	--	12.22	13.9	10.70
Helioscope	MBE	6.88	3.15	4.81	7.84	4.82	
	RMSE	11.37	8.77	9.64	11.02	9.19	
PVsyst	MBE	8.67	2.57	4.18	8.18	3.16	
	RMSE	12.72	8.84	9.63	11.70	8.55	
PV*SOL	MBE	0.16	-0.36	1.29	4.32	1.30	
	RMSE	8.59	8.13	8.39	8.52	7.89	
<b>C15</b>							
Homer	MBE	-2.71	--	3.79	6.35	2.28	
	RMSE	6.46	--	7.64	7.71	5.48	
Helioscope	MBE	3.00	-0.54	0.91	3.64	1.08	
	RMSE	6.15	4.83	6.25	4.94	4.56	
PVsyst	MBE	4.87	-0.84	0.54	4.29	-0.35	
	RMSE	7.32	5.35	6.6	5.79	4.89	
PV*SOL	MBE	-4.49	-4.93	-3.47	-0.76	-3.31	
	RMSE	7.39	7.27	7.46	4.38	5.98	
<b>C16</b>							
Homer	MBE	-2.87	--	2.97	5.42	2.38	
	RMSE	5.77	--	6.80	6.57	4.73	
Helioscope	MBE	2.74	-0.65	0.02	2.74	1.14	
	RMSE	5.28	3.78	5.67	3.89	3.54	
PVsyst	MBE	4.55	-1.13	-0.51	3.22	-0.45	
	RMSE	6.45	4.19	5.88	4.46	3.64	
PV*SOL	MBE	-4.78	-5.10	-4.43	-1.73	-3.31	
	RMSE	6.92	6.68	7.53	4.09	5.25	

**4. Conclusions**

In the present research article, the main consideration is PV module temperature. Four years of experimental investigations are inter-correlated with recent empirical/analytical estimations that are heavily used in international software. The main results showed that the module temperature values together with the incident solar irradiance are very effective in the performance of the module temperature estimations schemes. As the temperature and solar irradiance values increase other models become better, showing the situation that the derived methodologies are mainly climate/location dependent. It can be concluded that equation 4 (PV\*SOL) is better at low irradiance and ambient temperature values, while equation 2 (Helioscope) seems better overall. All these results are explained in detail.

Temperature differences between estimated and observed temperatures range between -30 °C and +30 °C (Figures. 2 and 3). The results show that the deviation of the module temperature varies significantly depending on the climatic circumstances. In different categories, the deviation between measured and estimated module temperature varies highly. For high-irradiance categories, Helioscope estimations of Poly-Si module temperature are highly correlated with the measurements. For category 9 the MBE deviation is only -0.01 and for category 16 the MBE deviation is 0.02.

The temperature estimation formula used by Homer software highly deviated for high irradiance values for μc-Si/a-Si module. For category 13 and category 14 and both the MBE and RMSE values attained > 11 RMSE and MBE values, meaning that the deviation is very high and the formula consistently over-estimates the μc-Si/a-Si module temperature.

Although the MBE estimations of PV\*SOL for low irradiance categories are low compared with other software's still the RMSE estimations can reach up to +6.39 in category 3 for Poly-Si, pointing that the deviation between the estimated and measured temperatures is too high at some time instants.

This research highlights the prospect of the present Solar Energy investments and gives very important clues to future achievements. Further research should be on the experimental and theoretical/analytical of solar energy on PV for a better renewable energy future.

## 5. Nomenclature

$\alpha$	Empirically-determined coefficient establishing the upper limit for module temperature at low wind speeds and high solar irradiance ( <i>dimensionless</i> )	$T_{amb}$	Ambient temperature ( $^{\circ}\text{C}$ )
$\alpha$	Absorptance coefficient ( <i>dimensionless</i> )	$T_{a,NOCT}$	Ambient temperature at NOCT ( $^{\circ}\text{C}$ )
$\alpha_p$	Temperature coefficient of power [ $\%/^{\circ}\text{C}$ ]	$T_{a,average}$	Average ambient temperature ( $^{\circ}\text{C}$ )
$b$	Empirically-determined coefficient establishing the rate at which module temperature drops as wind speed increases ( $\text{s/m}$ )	$T_{a,highest}$	Highest ambient temperature ( $^{\circ}\text{C}$ )
$\eta_{STC}$	Efficiency at STC ( <i>dimensionless</i> )	$T_{a,lowest}$	Lowest ambient Temperature ( $^{\circ}\text{C}$ )
$G_{NOCT}$	Irradiance at NOCT ( $\text{W/m}^2$ )	$T_c$	Cell temperature ( $^{\circ}\text{C}$ )
$G_t$	Solar radiation flux on module plane ( $\text{W/m}^2$ )	$T_{c,NOCT}$	Cell temperature at NOCT ( $^{\circ}\text{C}$ )
$G_{t,average}$	Average solar radiation flux on module plane ( $\text{W/m}^2$ )	$T_{c,STC}$	Cell temperature at standard test conditions ( $^{\circ}\text{C}$ )
$G_{t,highest}$	Highest solar radiation flux on module plane ( $\text{W/m}^2$ )	$U_0, U_1$	A coefficient describing the effect of the radiation on the module temperature ( $\text{W/m}^2^{\circ}\text{C}$ ), A coefficient describing the cooling by the wind ( $\text{Ws/m}^3^{\circ}\text{C}$ )
$k$	Installation Coefficient ( $^{\circ}\text{C}$ )	$WS$	Wind speed ( $\text{m/s}$ )
$p_{average}$	Average precipitation ( $\text{mm}$ )	$WS_{average}$	Average wind speed ( $\text{m/s}$ )
$p_{highest}$	Highest precipitation ( $\text{mm}$ )	$WS_{highest}$	Highest wind speed ( $\text{m/s}$ )
$\tau$	Transmittance coefficient ( <i>dimensionless</i> )	$I_t$	Irradiation ( $\text{W/m}^2$ )

## Acknowledgments

The authors would like to thank to Rasit Turan and Harun Tanik. The authors acknowledge the support given by Turkey Presidency of Strategy and Budget for constructing the outdoor testing facility [BAP-08.11.2015K121200]. Thanks to all the participants of ODTÜ-GÜNAM for establishing a scientific incorporation structure. The authors thank the editor and referees for their valuable feedback during the review and evaluation phase of the article.

## Author contribution

T.O., D.T., and M.S.Y did necessary maintenance operations for proper operation of solar panels. B.G.A. and T.O. planned and supervised the work, and D.T. and M.S.Y. did the calculations and plots for all software models. D.T. and M.S.Y wrote the introduction section, and B.G.A. and T.O. processed the data. All writers are contributed to the analysis, whereas D.T. and M.S.Y drafted the manuscript. B.G.A., T.O. depicted the results and worked on the manuscript. All authors discussed the results and commented on the manuscript.

## Declaration of ethical code

The authors of this article declare that the materials and methods used in this study do not require ethical committee approval and/or legal-specific permission.

## Conflicts of interest

The authors declare that there is no conflict of interest.

## References

- Akinoglu, B. G. (1991). A review of sunshine-based models used to estimate monthly average global solar radiation. *Renewable Energy*, 1(3–4), 479–497. [https://doi.org/10.1016/0960-1481\(91\)90061-S](https://doi.org/10.1016/0960-1481(91)90061-S)
- Aly, S. P., Ahzi, S., & Barth, N. (2019). Effect of physical and environmental factors on the performance of a photovoltaic panel. *Solar Energy Materials and Solar Cells*, 200(September 2018), 109948. <https://doi.org/10.1016/j.solmat.2019.109948>
- Atse, L., Waal, A. C. de, Schropp, R. E. I., Faaij, A. P. C., & Sark, W. G. J. H. M. van. (2017). Comprehensive characterisation and analysis of PV module performance under real operating conditions. *Progress In Photovoltaics: Research and Applications*, 25(2), 218–232. <https://doi.org/10.1002/pip.2848>
- Bañuelos-Ruedas, F., Angeles-Camacho, C., & Rios-Marcuello, S. (2010). Analysis and validation of the methodology used in the extrapolation of wind speed data at different heights. *Renewable and Sustainable Energy Reviews*, 14(8), 2383–2391. <https://doi.org/10.1016/j.rser.2010.05.001>
- Dubey, S., Sarvaiya, J. N., & Seshadri, B. (2013). Temperature dependent photovoltaic ( PV ) efficiency and its effect on PV production in the world a review. *Energy Procedia*, 33, 311–321. <https://doi.org/10.1016/j.egypro.2013.05.072>
- Duffie, J. A., Beckman, W. A., & McGowan, J. (1985). *Solar engineering of thermal processes*. <https://doi.org/10.1119/1.14178>
- Eckstein, J. H. (1990). *Detailed modelling of photovoltaic system components*. University of Wisconsin-Madison.
- Faiman, D. (2008). *Assessing the outdoor operating temperature of photovoltaic modules*. <https://doi.org/10.1002/pip.813>
- Folsom Labs. (2019). *HelioScope software*. <https://www.helioscope.com/>
- HOMER software. (2019). <https://www.homerenergy.com/>
- International renewable energy agency. (2020). *Renewable Capacity Statistics 2020*. <https://irena.org/publications/2020/Mar/Renewable-Capacity-Statistics-2020>
- Jaszczur, M., Teneta, J., Hassan, Q., Majewska, E., & Hanus, R. (2019). An experimental and numerical investigation of photovoltaic module temperature under varying environmental conditions. *Heat Transfer Engineering*, 42(3–4), 354–367. <https://doi.org/10.1080/01457632.2019.1699306>
- Jha, A., & Tripathy, P. P. (2019). Heat transfer modeling and performance evaluation of photovoltaic system in different seasonal and climatic conditions. *Renewable Energy*, 135, 856–865. <https://doi.org/10.1016/j.renene.2018.12.032>
- Karaveli, A. B., Ozden, T., & Akinoglu, B. G. (2018). Determining photovoltaic module performance and comparisons. *PVCon 2018 - International Conference on Photovoltaic Science and Technologies*, 18–22. <https://doi.org/10.1109/PVCon.2018.8523868>
- King, D. L., Boyson, W. E., & Kratochvil, J. A. (2004). Photovoltaic array performance model. In *Sandia Report No. 2004-3535* (Vol. 8, Issue November). <https://doi.org/10.2172/919131>
- Koehl, M., Heck, M., Wiesmeier, S., & Wirth, J. (2011). Modeling of the nominal operating cell temperature based on outdoor weathering. *Solar Energy Materials and Solar Cells*, 95(7), 1638–1646. <https://doi.org/10.1016/j.solmat.2011.01.020>
- Nikolaeva-Dimitrova, M., Kenny, R. P., Dunlop, E. D., & Pravattoni, M. (2010). Seasonal variations on energy yield of a-Si, hybrid, and crystalline Si PV modules. *Progress in Photovoltaics: Research and Applications*, 18(5), 311–320. <https://doi.org/10.1002/pip.918>
- Ozden, T., Akinoglu, B. G., & Kurtz, S. (2018). Performance and degradation analyses of two different pv modules in central anatolia. *PVCon 2018 - International Conference on Photovoltaic Science and Technologies*, 18–21. <https://doi.org/10.1109/PVCon.2018.8523880>

- Ozden, T., Carr, A. J., Geerligs, B. (L. J. ), Turan, R., & Akinoglu, B. G. (2020). One-year performance evaluation of two newly developed back-contact solar modules in two different climates. *Renewable Energy*, 145, 557–568. <https://doi.org/10.1016/j.renene.2019.06.045>
- Ozden, T., Karaveli, A., & Akinoglu, B. (2020). Fotovoltaik sistemlerde performans hesaplama modellerinin Ankara (Orta Anadolu) için karşılaştırılması. *European Journal of Science and Technology*, 18, 54–60. <https://doi.org/10.31590/ejosat.653272>
- Ozden, T., Tolgay, D., & Akinoglu, B. G. (2018). Daily and monthly module temperature variation for 9 different modules. *PVCon 2018 - International Conference on Photovoltaic Science and Technologies*. <https://doi.org/10.1109/PVCon.2018.8523878>
- Ozden, T., Tolgay, D., Yakut, M. S., & Akinoglu, B. G. (2020). An extended analysis of the models to estimate photovoltaic module temperature. *Turkish Journal of Engineering*, 4(4), 183–196. <https://doi.org/10.31127/tuje.639378>
- Peel, M. C., Finlayson, B. L., & McMahon, T. A. (2007). Updated world map of the Köppen-Geiger climate classification. *Hydrology and Earth System Sciences*, 11(5), 1633–1644. <https://doi.org/10.5194/hess-11-1633-2007>
- PVsystem. (2019). *PVsystem PV Software*. <https://www.pvsystem.com>
- Radziemska, E. (2003). The effect of temperature on the power drop in crystalline silicon solar cells. *Renewable Energy*, 28, 1–12. [https://doi.org/10.1016/S0960-1481\(02\)00015-0](https://doi.org/10.1016/S0960-1481(02)00015-0)
- Rahman, M. M., Hasanuzzaman, M., & Rahim, N. A. (2015). Effects of various parameters on PV-module power and efficiency. *Energy Conversion and Management*, 103, 348–358. <https://doi.org/10.1016/j.enconman.2015.06.067>
- Ross, R. G., & Smokler, M. I. (1986). *Electricity from photovoltaic solar cells: Flat-Plate Solar Array Project final report*. [https://www2.jpl.nasa.gov/adv\\_tech/photovol/ppr\\_86-90/FSA%20Final%20Rpt%20VII%20-%20Encapsulation.pdf](https://www2.jpl.nasa.gov/adv_tech/photovol/ppr_86-90/FSA%20Final%20Rpt%20VII%20-%20Encapsulation.pdf)
- Rubel, F., Brugger, K., Haslinger, K., & Auer, I. (2017). The climate of the European Alps: Shift of very high resolution Köppen-Geiger climate zones 1800-2100. *Meteorologische Zeitschrift*, 26(2), 115–125. <https://doi.org/10.1127/metz/2016/0816>
- Sandnes, B., & Rekstad, J. (2002). A photovoltaic/thermal (PV/T) collector with a polymer absorber plate. Experimental study and analytical model. *Solar Energy*, 72(1), 63–73. [https://doi.org/10.1016/S0038-092X\(01\)00091-3](https://doi.org/10.1016/S0038-092X(01)00091-3)
- Shen, L., Li, Z., & Ma, T. (2020). Analysis of the power loss and quantification of the energy distribution in PV module. *Applied Energy*, 260(November 2019), 114333. <https://doi.org/10.1016/j.apenergy.2019.114333>
- Skoplaki, E., Boudouvis, A. G., & Palyvos, J. A. (2008). A simple correlation for the operating temperature of photovoltaic modules of arbitrary mounting. *Solar Energy Materials and Solar Cells*, 92(11), 1393–1402. <https://doi.org/10.1016/j.solmat.2008.05.016>
- Tuncel, B., Ozden, T., Balog, R. S., & Akinoglu, B. G. (2020). Dynamic thermal modelling of PV performance and effect of heat capacity on the module temperature. *Case Studies in Thermal Engineering*, 22(August), 100754. <https://doi.org/10.1016/j.csite.2020.100754>
- Twidell, J., & Weir, T. (2015). *Renewable Energy Resources* (3rd Edition, Ed.). Taylor Francis. <https://doi.org/10.4324/9781315766416>
- Valentin software. (2019). *PV\*SOL*. <https://valentin-software.com/en/products/pvsol-premium/>
- Ye, J., Reindl, T., & Luther, J. (2012). Seasonal variation of PV module performance in tropical regions. *Conference Record of the IEEE Photovoltaic Specialists Conference*, 2406–2410. <https://doi.org/10.1109/PVSC.2012.6318082>
- Ye, Z., Nobre, A., Reindl, T., Luther, J., & Reise, C. (2013). On PV module temperatures in tropical regions. *Solar Energy*, 88, 80–87. <https://doi.org/10.1016/j.solener.2012.11.001>